Bandwidth control of paired photons generated in monolithic Bragg reflection waveguides

Payam Abolghasem,[1] Martin Hendrych,[2] Xiaojuan Shi,[2] Juan P. Torres,[2] and Amr S. Helmy[1,*]

[1]*The Edward S. Rogers Sr. Department of Electrical and Computer Engineering, University of Toronto, 10 King's College Road, Toronto, Ontario M5S 3G4, Canada*

[2]*ICFO-Institut de Ciencies Fotoniques, Mediterranean Technology Park, Universitat Politecnica de Catalunya 08860 Castelldefels (Barcelona), Spain*

**Corresponding author: a.helmy@utoronto.ca*

Received February 8, 2009; revised May 31, 2009; accepted June 1, 2009; posted June 5, 2009 (Doc. ID 107297); published June 26, 2009

Bragg reflection waveguides are considered as monolithic sources of frequency correlated photon pairs generated using spontaneous-parametric down-conversion in a $Al_xGa_{1-x}As$ material system. The source described here offers unprecedented control over the process bandwidth, enabling bandwidth tunability between 1 nm and 450 nm while using the same wafer structure. This tuning is achieved by exploiting the powerful control over the waveguide dispersion properties afforded by the phase-matching technique used. The offered technology provides a route for realizing electrically pumped, monolithic photon pair sources on a chip with versatile characteristics. © 2009 Optical Society of America

OCIS codes: 230.1480, 190.2620, 270.0270, 230.7370.

An increasing number of quantum optics applications, ranging from quantum information processing and quantum communications [1] to quantum metrology and quantum imaging [2], show enhanced capabilities due to the use of biphotons with quantum frequency correlations (*entanglement*). The successful technological implementation of these new applications, primarily, depends on efficient and robust sources that offer a high flux rate of paired photons while they allow tailoring the biphoton's quantum state for a particular application.

Spontaneous-parametric down-conversion (SPDC) is the most popular method for the generation of photon pairs with entangled properties [3]. The SPDC process is often implemented in bulk crystals using a solid-state laser source as pump. The use of these crystals does not generally offer significant control over the spatiotemporal properties of the down-converted photons. Using tilted pulses [4] or chirping the domains of the nonlinearity in quasi-phase-matched configurations [5] can provide control over the frequency-temporal characteristics. In addition to this, guided-wave alternatives can improve the spatial characteristics [6].

A new class of biphoton sources based on compound semiconductors, particularly $Al_xGa_{1-x}As$ elements, has received some attention in the literature [7]. Such devices are promising in an integrated platform where the frequency down-converting element is monolithically integrated with a diode laser pump. Despite large second-order nonlinearity of compound semiconductors, phase matching (PM) in these materials is not trivial owing to the lack of birefringence. Engineering techniques based on quasi-phase matching and artificial birefringence are widely used to attain phase-matching in III-V materials. Another scheme, employed here, uses Bragg reflection waveguides (BRWs) where exact PM among the frequencies involved in the nonlinear process can be attained [8].

In a SPDC process, tailoring temporal correlation or spectral bandwidth of photon pairs is essential for practical purposes. Certain applications demand short correlation times. Examples include the enhancement of the accuracy of protocols for quantum positioning and timing [9], or the enhancement of sensitivity due to quantum illumination [2]. Other applications benefit from photon pairs with large temporal correlation or narrow spectral bandwidth. Examples include efficient atom–photon interfaces, or long-haul transmission of entangled photons in optical fibers for quantum communication [10].

In an integrated source of down-converted photons dispersion properties can be tailored using material dispersion, waveguide dispersion, or a combination of both mechanisms [11,12]. Most widely used approaches for controlling material dispersion rely on temperature and electro-optic tuning, which are, in general, weak effects in a $Al_xGa_{1-x}As$ system. However, significant control over waveguide dispersion is available through proper choice of the ridge width W, which could be simply implemented using standard lithographic techniques. The dependency of waveguide dispersion on the ridge dimension is more pronounced in subwavelength ridges, where highly confined optical modes are established as a result of large index contrast between the waveguide's core and claddings [13,14]. Here, we employ the strong dependency of waveguide dispersion on the ridge size as an effective mechanism for controlling dispersion properties of photon pairs in a monolithically integrated source.

A representative ridge BRW along with typical intensity profiles of the pump and down-converted photons is schematically illustrated in Fig. 1. The periodic claddings consists of 12 periods of $Al_{0.40}Ga_{0.60}As/Al_{0.90}Ga_{0.10}As$ with associated thicknesses of 89 nm/200 nm. The core is $Al_{0.65}Ga_{0.35}As$ with a thickness of 246 nm. The material indices of the $Al_xGa_{1-x}As$ elements were derived using the

0146-9592/09/132000-3/$15.00

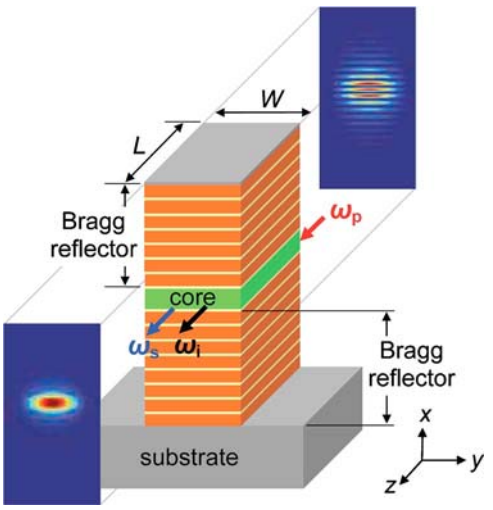

Fig. 1. (Color online) Schematic of a typical BRW with intensity profiles of TM-polarized pump (ω_p) and TE-polarized down-converted photons (ω_s, ω_i) in type-I phase matching.

model proposed in [15] at the temperature $T=293$ K. The sample length was taken as $L=3$ mm. Dispersion values of different orders were calculated using standard finite-difference techniques and were confirmed using mathematical fitting tools.

We assume that the pump beam is a cw source with frequency ω_p^0, while the frequencies of the signal and idler photons are written $\omega_s=\omega_s^0+\Omega_s$ and $\omega_i=\omega_i^0+\Omega_i$, respectively, where ω_s^0 and ω_i^0 are the corresponding central angular frequencies, and Ω_s and Ω_i are the associated angular frequency deviations. The quantum state at the output facet of the nonlinear waveguide can be expressed as $|\psi\rangle=\int\int d\Omega_s d\Omega_i \Phi(\Omega_s,\Omega_i)\Gamma(\Omega_s,\Omega_i)|\omega_s^0+\Omega_s\rangle|\omega_i^0-\Omega_s\rangle$, where $\Phi(\Omega_s,\Omega_i)=E_p(\Omega_s+\Omega_i)\mathrm{sinc}(\Delta_k L/2)\exp(is_k L/2)$ is the biphoton spectral amplitude, E_p is the pump spectrum, L is the sample length, $s_k=k_p(\omega_p^0)+k_s(\omega_s)+k_i(\omega_i)$, and $\Delta_k=k_p(\omega_p^0)-k_s(\omega_s)-k_i(\omega_i)$ is the phase mismatch. We have verified numerically that the spatial overlap $\Gamma(\Omega_s,\Omega_i)$ of the interacting modes is close to unity for all the frequencies.

Broadband SPDC is attainable in type-I phase matching where TM-polarized pump photons generate photon pairs with TE polarization state. The effects of the waveguide design parameters on the SPDC spectrum can be understood by performing a Taylor expansion of Δ_k around the central frequencies. It follows that the SPDC phase mismatch is predominantly determined by the group velocity dispersion (GVD) of the signal/idler, so that, ignoring higher-order terms, $\Delta_k \approx -D_s\Omega_s^2$, where $D_s=d^2k_s/d\Omega_s^2$ is evaluated at the corresponding central frequency. To maximize the process bandwidth, the waveguide design should satisfy the condition $D_s\approx 0$. We monitor the pump wavelength for exact PM, λ_p, and, D_s as functions of the ridge width W over the range of 0.6 μm–4.0 μm.

The results are illustrated in Figs. 2(a) and 2(b), where $D_s=-7.6\times10^{-4}$ ps^2/m was obtained for the design point D_1, which corresponds to $(W,\lambda_p)=(677\text{ nm},741\text{ nm})$. The joint spectral intensity $|\Phi(\Omega_s,\Omega_i)|^2$ of the source is illustrated in Fig. 2(c). The FWHM bandwidth $\Delta\nu_{\mathrm{FWHM}}$ is estimated to be 61 THz ($\approx$456 nm). The phase of the spectral amplitude $s_k L/2$ is shown in Fig. 2(d). It is instructive to note the flat phase response around the degeneracy point ($\Omega_s=0$), which is expected as a result of the dependency of s_k on Ω_s (expressed by a fourth-order polynomial). This large bandwidth can be translated into an extremely narrow correlation time. The temporal shape of the correlation between signal and idler photons is given by the Fourier transform of $\Phi(\Omega_s,\Omega_i)$. This translates to $\approx$15 fs for the temporal delay between the arrival times of the down-converted photons for D_1. Comparable temporal correlations (23 fs) can be achieved by choosing an adequate nonlinear material and working at a specific wavelength and PM conditions [16].

To investigate the potential of the proposed design in reducing the SPDC bandwidth, we further examined the biphoton generation in a type-II phase-matching scheme where a TE-polarized pump generates a pair of a signal and an idler with TE and TM polarization states. In this case, Δ_k is predominantly determined by the group velocity mismatch (GVM) between signal and idler and is approximated as $\Delta_k \approx (N_i-N_s)\Omega_s$, where $N_j=dk_j/d\Omega_j$ ($j=i,s$). The minimization of the process bandwidth requires N_i-N_s to be maximum. We thus monitored the variation of λ_p and N_i-N_s as functions of the ridge width over the range of 0.375 μm–4.0 μm, as shown in Figs. 3(a) and 3(b), respectively. From the figures, the maximum value of $N_i-N_s=-2.92$ ns/m was obtained for the design D_2 with $(W,\lambda_p)=(375\text{ nm},944\text{ nm})$. The joint spectral intensity is illustrated in Fig. 3(c), where the SPDC bandwidth of $\Delta\nu_{\mathrm{FWHM}}=101$ GHz ($\approx$1.2 nm) was obtained. The phase of $\Phi(\Omega_s,\Omega_i)$ is illustrated in Fig. 3(d), where the linear phase response confirms the

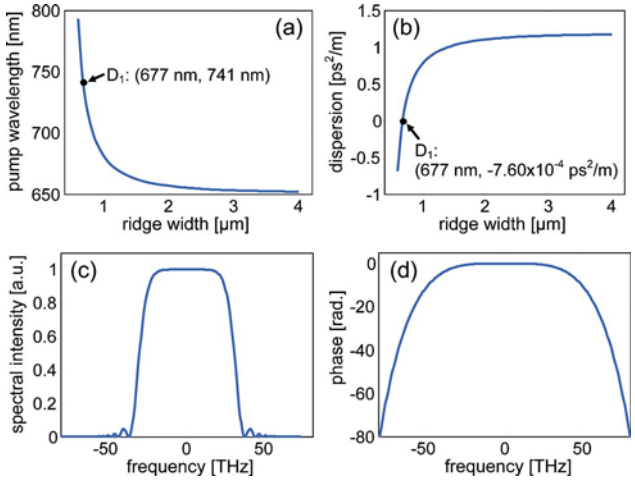

Fig. 2. (Color online) (a) Pump wavelength (λ_p) versus ridge width (W), and (b) the group velocity dispersion of signal (D_s) versus ridge width in type-I phase-matched BRW of Fig. 1. (c) Normalized joint spectral intensity, and (d) phase of spectral amplitude of biphotons for the design D_1 with $\Delta\nu_{\mathrm{FWHM}}\approx 61$ THz ($\approx$456 nm).

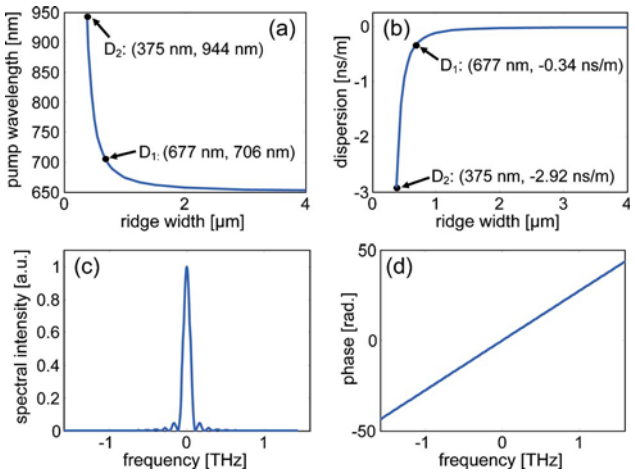

Fig. 3. (Color online) (a) Pump wavelength (λ_p) versus ridge width (W), and (b) the GVM between signal and idler ($N_i - N_s$) versus ridge width in type-II phase-matched BRW of Fig. 1. (c) Normalized joint spectral intensity, and (d) phase of spectral amplitude of biphotons for the design D_2 with $\Delta\nu_{\mathrm{FWHM}} \approx 101$ GHz (≈ 1.2 nm).

linearity of s_k on Ω_s in type-II PM. The obtained temporal correlation of the biphoton was 10 ps.

Also, it would be interesting to verify the SPDC bandwidth offered by the design D_1 using type-II PM. From simulation, $N_i - N_s$ was -0.34 ns/m for $\lambda_p = 706$ nm. The bandwidth obtained is $\Delta\nu_{\mathrm{FWHM}} = 869$ GHz (≈ 5.7 nm) with a temporal correlation of 1.2 ps. Note that that can be achieved by simply rotating the polarization of the pump beam. The comparison between the estimated bandwidths in type-I and type-II PM indicates that the proposed structure is capable of controlling the SPDC bandwidth over 2.5 orders of magnitudes. Such flexibility is attractive for the development of integrated photon pair sources, where large tunability over the temporal correlation of biphotons is desired.

It should be noted that no theoretical limitation exists on the attainable upper and lower limits of the spectral bandwidth. Instead, the limitations were posed by the practical considerations of designing the structures discussed. For example, for narrowband SPDC, larger $N_i - N_s$, hence smaller bandwidth, is possible by reducing the ridge width. However, this would degrade the conversion efficiency of the process as the TE-polarized down-converted photons will experience greater losses inside the waveguide. A possible route for further broadening the SPDC spectrum in type-I PM is operating in a regime with lower material dispersion. For both narrowband and broadband sources, the fabrication step in fabricating the waveguides is expected to be challenging because of the small ridge sizes. The sharp slopes observed in Figs. 2(b) and Fig. 3(b) denote large design sensitivity to fabrication tolerances which can be compensated for partly through temperature tuning, or electro-optically.

In summary, Bragg reflection waveguides are used to achieve phase matching for spontaneous-parametric down-conversion in monolithic $Al_xGa_{1-x}As$ waveguides. Through the dispersion control afforded by this technique, bandwidth tunablity between 1 nm and 450 nm could be achieved using the same vertical wafer structure. The tuning was achieved by patterning waveguides with different ridge widths and also by utilizing both type-I and type-II phase-matching conditions. This technology offers a promising route for realization of electrically pumped, monolithic photon-pair sources on a chip with versatile characteristics.

This work was supported by the European Commission (Qubit Applications, contract 015848) and the Government of Spain [Consolider Ingenio 2010 (QOIT) CSD2006-00019 and FIS2007-60179]. This work was supported by an ICFO-OCE (Ontario Centers of Excellence) Collaborative Research Program.

References

1. D. Bouwmeester, A. K. Ekert, and A. Zeilinger, *The Physics of Quantum Information: Quantum Cryptography, Quantum Teleportation, Quantum Computation* (Springer, 2000).
2. S. Lloyd, Science **321**, 1463 (2008).
3. Y. Shih, Rep. Prog. Phys. **66**, 1009 (2003).
4. M. Hendrych, M. Mičuda, and J. P. Torres, Opt. Lett. **32**, 2339 (2007).
5. M. B. Nasr, S. Carrasco, B. A. E. Saleh, A. V. Sergienko, M. C. Teich, J. P. Torres, L. Torner, D. S. Hum, and M. M. Fejer, Phys. Rev. Lett. **100**, 183601 (2008).
6. K. Banaszek, A. B. U'Ren, and I. Walmsley, Opt. Lett. **26**, 1367 (2001).
7. X. Caillet, V. Berger, G. Leo, and S. Ducci, J. Mod. Opt. **56**, 232 (2009).
8. A. S. Helmy, Opt. Express **14**, 1243 (2006).
9. A. Valencia, G. Scarcelli, and Y. H. Shih, Appl. Phys. Lett. **85**, 2655 (2004).
10. S. Sauge, M. Swillo, S. Alber-Seifried, G. B. Xavier, J. Waldeback, M. Tengner, D. Ljunggren, and A. Karlsson, Opt. Express **15**, 6926 (2007).
11. M. G. Raymer, J. Noh, K. Banaszek, and I. A. Walmsley, Phys. Rev. A **72**, 023825 (2005).
12. Z. D. Walton, A. V. Sergienko, B. E. A. Saleh, and M. C. Teich, Phys. Rev. A **70**, 052317 (2004).
13. J. Meier, W. S. Mohammed, A. Jugessur, L. Qian, M. Mojahedi, and J. S. Aitchison, Opt. Express **15**, 12755 (2007).
14. M. A. Foster, A. C. Turner, M. Lipson, and A. L. Gaeta, Opt. Express **16**, 1300 (2008).
15. S. Gehrsitz, F. K. Reinhart, C. Gourgon, N. Herres, A. Vonlanthen, and H. Sigg, Appl. Phys. **87**, 7825 (2000).
16. B. Dayan, A. Pe'er, A. A. Friesem, and Y. Silberberg, Phys. Rev. Lett. **93**, 023005 (2004).